Food Eng. Prog.
Vol. 23, No. 3. pp. 171~177 (2019.8)
DOI https://doi.org/10.13050/foodengprog.2019.23.3.171
ISSN 1226-4768 (print), ISSN 2288-1247 (online)

산업식품공학
Food Engineering Progress

Degradation of Benzo[α]pyrene in Roasted Oil Seeds by Corona Discharge Plasma Jet

Taehoon Lee, Pradeep Puligundla, and Chulkyoon Mok*

Department of Food Science and Biotechnology, Gachon University

Abstract

Benzo[α]pyrene (BaP), a carcinogenic polycyclic aromatic hydrocarbon, is ubiquitous in nature. It is generally found in heat-treated foods like roasted sesame seeds. BaP degradation has attracted attention due to the recalcitrant nature of BaP. In this study, corona discharge plasma jet (CDPJ) was used to degrade BaP on glass slides and in food materials. The plasma discharges were generated using air as working gas under atmospheric pressure conditions and at different currents (1.00, 1.25, and 1.50 A). Optimal BaP degradation was observed upon using CDPJ generated at 1.50 A current and at 15 mm sample-to-electrode distance (STED). Under these conditions, initial BaP concentration on slides was reduced maximally by 87.09% in 30 min. The degradation kinetics were well-fitted by Weibull tail model compared with others. In food commodities (roasted sesame and perilla seeds), the average levels of BaP degradation ranged between 32.96-45.90% following CDPJ treatment for 30 min.

Key words: benzo[α]pyrene, degradation, corona discharge plasma jet, kinetic modeling

Introduction

The incomplete pyrolysis or combustion of organic materials (e.g., coal, oil, gas, wood and garbage) at temperatures between 300 and 600°C results in the formation of benzo[α]pyrene (BaP), a carcinogenic polycyclic aromatic hydrocarbon. The presence of BaP is ubiquitous; ranging from coal tar to tobacco smoke to heat-treated foods. In foods, BaP is induced by heat treatments such as grilling or roasting, and therefore its formation is commonly observed in smoked/grilled meats and roasted seeds. The formation of BaP during roasting of sesame seeds has been shown in earlier studies (Cheng et al., 2015; Lee et al., 2019). The International Agency for Research on Cancer has categorized BaP as a Group 1 carcinogen; BaP-induced tumorigenesis in experimental animals has been well established (IARC, 2012). In addition, the US Environmental Protection Agency has classified as priority pollutant due to its acute toxicity, carcinogenicity and known or suspected teratogenicity (Kot-Wasik et al., 2004). BaP toxicity is mediated by oxidative metabolism to reactive intermediates that interact with macromolecules leading to alterations in target cell structure and function (Miller & Ramos, 2001). BaP is metabolized in cells by cytochrome P450 to BaP diol-epoxides or BPDE that bind to DNA covalently, resulting in the formation of DNA adducts and eventually cancer initiation (Fu & Xia, 2016).

Due to its ubiquitous distribution and toxicity, BaP detoxification in foods or the remediation of BaP-contaminated sites has received considerable attention. However, due to its recalcitrant nature, BaP degradation cannot be achieved easily. Different methods such as volatilization, photo-oxidation, chemical oxidation, bioaccumulation, adsorption on sediment particles, microbiological transformation and degradation, etc., have been used for the degradation and elimination of PAHs including BaP from the environment (Wilson & Jones, 1993). But, conventional oxidants (e.g., Cl_2, ClO_2 and $KMnO_4$) suffer from inherent disadvantages such as the inability to produce highly reactive species, low reaction rate, and more specific with regard to the types of organic molecules that can be oxidized. In addition, biodegradability of PAHs is low. Hence, there has been growing interest in the use of advanced oxidation processes (AOPs), which utilize oxidants such as ozone (O_3) and Fenton's reagent, for PAHs degradation. Electrochemically generated O_3 has been shown to be effective in degrading and detoxifying BaP (Ottinger et al., 1999). In another study, in the remediation of PAH (including BaP) from spiked and coal tar-contaminated soils, combined ozonation/biodegradation treatments have been shown to be effective

*Corresponding author: Chulkyoon Mok, Department of Food Science & Biotechnology, Gachon University, Seongnam-si, Gyeonggi-do 13120, Republic of Korea.
Tel: 82-31-750-5403
E-mail : mokck@gachon.ac.kr
Received July 15, 2019; revised August 20, 2019; accepted August 21, 2019

(Nam & Kukor, 2000). The effectiveness of Fenton's reagent (a solution of hydrogen peroxide with ferrous iron as a catalyst) for the degradation of BaP in water matrices has been shown (Homem et al., 2009).

Non-thermal plasma (NTP) or cold plasma represents one of the most promising sources of oxidants. NTPs can generate different types of reactive oxygen species (ROS) (e.g., hydroxyl ($HO^{\bullet}$), hydroperoxyl ($HO2^{\bullet}$), ozone (O_3)) and reactive nitrogen species (RNS) (e.g., nitric oxide (NO), peroxynitrite ($ONOO^-$), nitrite (NO_2^-), nitrate (NO_3^-)), which have a higher oxidation potential to react with organic molecules (Attri et al., 2016). Effective degradation of organic dyes, namely methylene blue, methyl orange and Congo red, following treatments with two needle-type atmospheric pressure plasma jets (APPJs), an indirect (ID-APPJ) and a direct (D-APPJ), has been shown (Attri et al., 2016). Corona plasma discharges are known to produce reactive species such as electrons, oxygen ions and excited neutrals (Choi et al., 2017). Hence, in the present study, corona discharge plasma jet (CDPJ) generated using air under atmospheric pressure conditions was used to degrade BaP on glass slides and modelled its degradation kinetics. In addition, our study investigated CDPJ degradation of BaP in food commodities, namely roasted sesame and perilla seeds and their oils.

Materials and Methods

Chemicals and reagents

Benzo[α]pyrene having ≥96% purity (HPLC grade) was purchased from Sigma-Aldrich Co. (St. Louis, MO, USA). LC-grade water and HPLC-grade acetonitrile were obtained from J. T. Baker (Phillipsburg, NJ, USA) and Duksan Pure Chemical Co., Ltd. (Ansan, Korea), respectively. All other chemicals used were of analytical grade quality.

Food commodities

Food commodities used in this study, namely sesame and perilla seeds, were procured from a local store in Yongin-si, Gyeonggi-do, Korea.

Corona discharge plasma jet (CDPJ)

CDPJ generation system, which was designed by the authors, consisted of power supply (output voltage: 20 kV DC; frequency: 58 kHz), electrode assembly, air blower and sample treatment plate, as given in our earlier studies (Kim et al., 2015; Puligundla et al., 2017). The components of the system are illustrated in Fig. 1. A streamer-type corona discharge in air was generated between electrodes (tungsten) under atmospheric pressure conditions. A centrifugal air blower (Ventur Tekniska, Goteborg, Sweden) with a constant speed (3312 rpm) was used for plasma jet creation. The plasma emission slit in electrode housing unit measured 6 × 35 mm. Air velocity at the tip of the electrodes was 2.5 m/s, and a 5 mm inter-electrode gap was maintained.

Degradation of benzo(a)pyrene on glass slides using CDPJ

BaP in acetonitrile (10 ppm) test samples were prepared. Drops (10 μL each) of the sample were taken onto glass slides (76 × 26 mm) (a drop on each slide) spread and dried under a laminar air flow for 10 min. Thereafter, the slides were individually placed on the sample treatment plate and treated using CDPJ generated under different input currents (1.00, 1.25, and 1.50 A) and at different sample-to-electrode distances (STED) (15, 25, and 30 mm) for predetermined durations (5, 10, 15, 20, 25, and 30 min). Immediately following plasma treatment, residual BaP from the glass surfaces were recovered using acetonitrile rinse (1 mL for each slide).

Quantitation of benzo(a)pyrene

High performance liquid chromatography (HPLC) system (Dionex Ultimate 3000, Thermo Scientific, San Jose, CA, USA) was used for the quantification of BaP before and after the plasma treatment according to the method described previously (Chen et al., 2012). Due to the non-polar nature of BaP, a C_{18} column (250 × 4.6 mm ID, 5 μm particle size) was

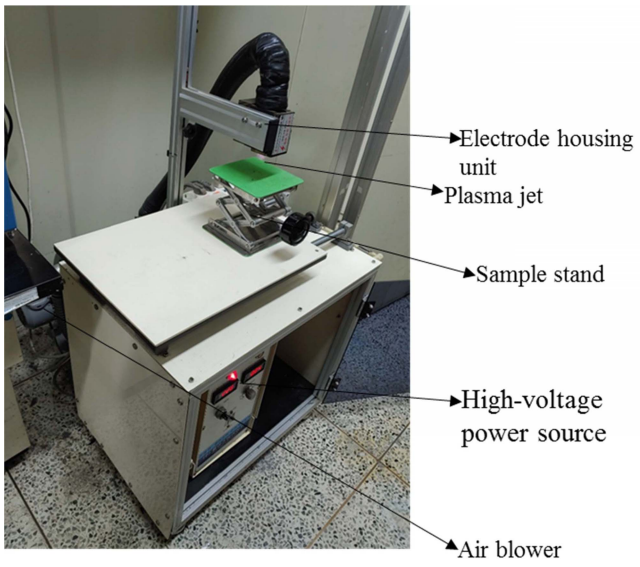

Fig. 1. The components of CDPJ generation system.

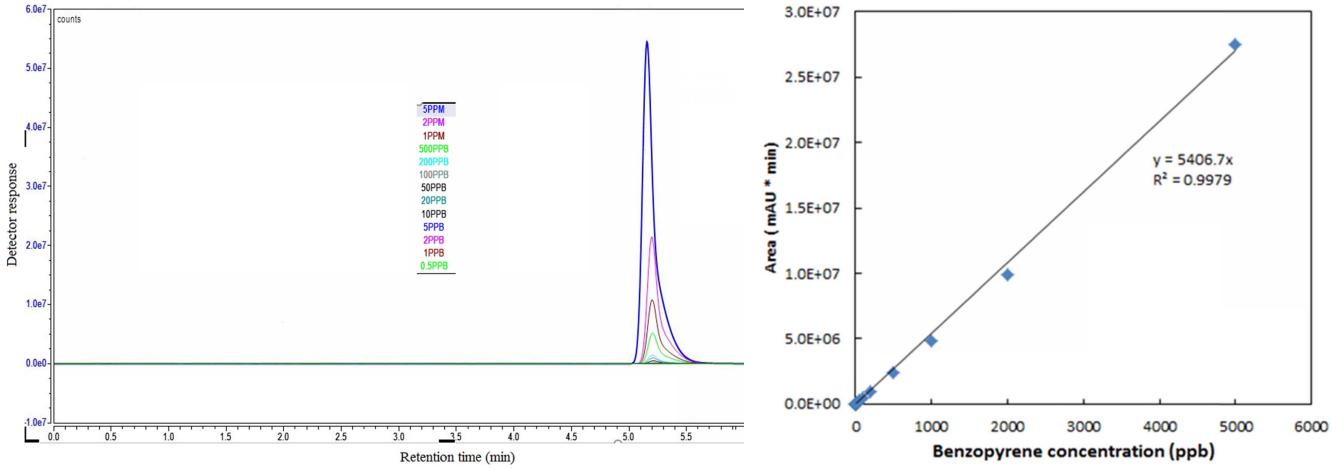

Fig. 2. HPLC chromatograms for different concentrations of BaP and calibration curve for BaP.

used with acetonitrile: water (90:10) as the mobile phase with a flow rate of 1.5 mL/min at the column temperature of 25°C. Residual BaP containing samples were filtered using 0.22-μm PVDF membrane syringe filters (SmartPor, Woongki Science Co., Ltd, Seoul, Korea) before being injected into the column. The amount of sample injected was maintained at 10 μL. BaP detection was performed by using a fluorescence detector at an excitation wavelength of 361 nm and an emission wavelength of 405 nm. BaP concentration was calculated from the peak area using a standard curve. HPLC chromatograms for different concentrations of BaP and calibration curve for BaP are shown in Fig. 2.

Degradation amount and modeling of degradation

BaP concentration was calculated from the detector response to injected samples using a standard calibration curve. BaP degradation was calculated based on the initial concentration of BaP using the following equation:

$$\text{Degradation (\%)} = (1 - C_t/C_0) \times 100$$

where C_t = the concentration of BaP at time (t), and C_0 = initial concentration of BaP.

For modeling the degradation kinetics of BaP, the appropriateness of the following models was compared.

Log-linear model (Bigelow & Esty, 1920):

$$\log C = \log C_0 - \frac{k_{max} \cdot t}{\ln 10}$$

Log-linear tail model (Geeraerd et al., 2000):

$$\log C = \log[(C_0 - C_{res}) \times e^{-k_{max} \cdot t} + C_{res}]$$

Weibull model (Mafart et al., 2002):

$$\log C = \log C_0 - \left(\frac{t}{\delta}\right)^m$$

Weibull-tail model (Albert and Mafart, 2005):

$$\log C = \log\left[(C_0 - C_{res}) \times 10^{-\left(\frac{t}{\delta}\right)^m} + C_{res}\right]$$

Where, C = remaining concentration (%)

C_0 = initial concentration (%)

C_{res} = residual concentration (%)

k_{max} = first order decrease rate constant (1/min)

m = curve shape factor

δ = initial decimal reduction time (min)

BaP in food materials and its degradation by CDPJ

BaP in food samples, namely sesame and perilla seeds, was induced by their roasting. The roasting was allowed up to a final roasting temperature of 220°C for regular roasted sesame (RRS) seeds and up to 245°C for over roasted sesame (ORS) seeds. In the case of perilla seeds, final roasting temperatures were 210°C and 230°C for regular roasted perilla (RRP) seeds and over roasted perilla (ORP) seeds, respectively.

Roasting-induced BaP in RRS, ORS, RRP and ORP seeds was degraded using CDPJ. Treatment conditions similar to that of BaP degradation on glass slides were used for BaP degradation in RRS, ORS, RRP and ORP seeds. About 10 g of each of the seed samples was exposed to CDPJ at predetermined time intervals (0, 10, 20, and 30 min). Soon after treatment, the samples were extracted with hexane and analyzed to determine the level of BaP degradation.

The concentrations of BaP in oils extracted from the roasted seeds (before and after CDPJ treatment) were also studied. For oil extraction, 10 g sample of each of the RRS, ORS, RRP and

ORP seeds was subjected to mechanical pressing using a screw press or expeller (HD-333, Ggaebaksa. Co., Seoul, Korea) and extracted with 100 mL of hexane.

Quantification of BaP in food samples

Roasting-induced BaP in the seeds was quantified by the aforementioned method. The following procedure was used in the preparation of samples for the HPLC analysis. Briefly, 10 g of ground seed (flour) /10 g seed oil was mixed with 100 mL of ethyl ether, and the mixture was incubated for 12 h. Then, the ethyl ether of the extract was evaporated, followed by the addition of 100 mL of hexane. The resultant mixture was filtered using Whatman No. 2 filter paper, and the filtrate was transferred to a separatory funnel (I) and 50 mL of N, N-dimethylformamide: water (9: 1, v/v) was added to the funnel and shaken vigorously. The N, N-dimethylformamide-water layer was then transferred to another separatory funnel (II). Then, 25 mL of N, N-dimethylformamide-water was added to the hexane layer of the separatory funnel (I), and the mixture was shaken well and the N, N-dimethylformamide-water layer was added to the separatory funnel (II). The rest of the procedure was the same as that described in our previous study (Lee et al., 2019).

Statistical analysis

All treatments were performed in triplicate, and the results are represented as mean±standard deviation. Statistical analysis of data was performed using SAS statistical software package (version 9.2, SAS Institute Inc., Cary, NC, USA). Data were analyzed by one-way analysis of variance (ANOVA), followed by Duncan's multiple range test at α= 0.05.

Results and Discussion

Effect of sample-to-electrode distance and current on BaP degradation

Sample-to-electrode distance influenced the degradation of BaP on glass slides. An increase of the distance linearly decreased the efficiency of BaP degradation (Fig. 3). A steep reduction by up to 50% of initial BaP concentration was observed upon CDPJ (generated using plasma current of 1.5 A) treatment within 1-2 min, at all tested STED (15, 25, and 35 mm). Thereafter, the rate of degradation was relatively slowed, ≥85% degradation was noted within 30 min of CDPJ treatment at 15 and 25 mm STED. At the 15 mm distance, residual BaP levels on glass slides following CDPJ treatment (for 30 min) at 1.00 A, 1.25 A, and 1.50 A were 15.10%, 14.86%, and 12.91%, respectively. At the 25 mm distance, residual BaP levels were 15.36%, 14.91%, and 13.11% using CDPJ at 1.00, 1.25, and 1.50 A current, respectively. On the other hand, at a STED of 35 mm, BaP degradation efficiency was relatively low; the levels of residual BaP were 20.24, 18.02 and 14.77% using CDPJ at 1.00, 1.25, and 1.50 A current, respectively. These results indicated that optimal conditions for BaP degradation were CDPJ generation at 1.50 A current and treatment at 15 mm STED.

Kinetics of BaP degradation

The applicability of selected models, namely log-linear, log-linear tail, Weibull, and Weibull tail, to explain CDPJ-induced BaP degradation was tested. Among these models, Weibull tail model was found to be the best model. The Weibull tail model fitted well to the degradation data. This conclusion was based on based on the values of SSE (sum of squared errors) RMSE (root mean squared error), and R^2 (coefficient of determination

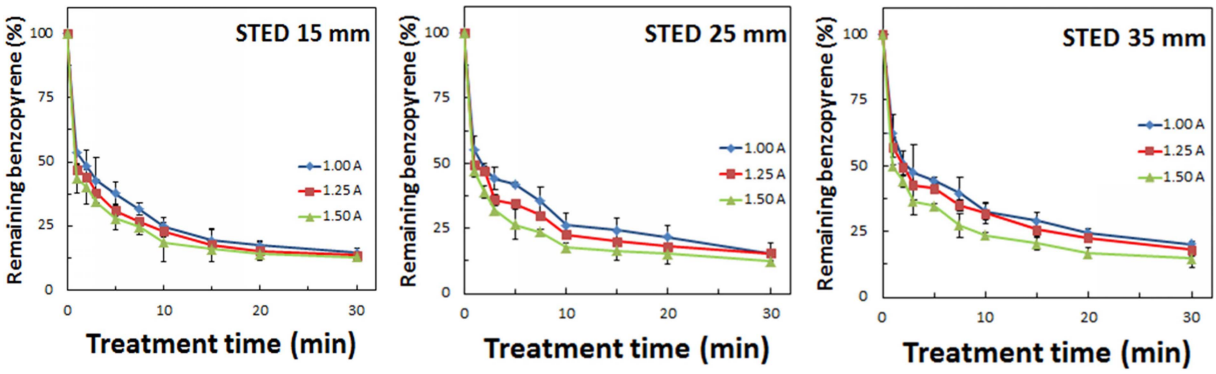

Fig. 3. The pattern of BaP degradation by CDPJ at different input currents and sample-to-electrode distances (STED).

or fit index). A relatively high R^2 value (close to 1) and low SSE and RMSE values for Weibull tail model indicates that the model is the best-fitting model compared with others (Table 1).

The same Weibull tail model was used to explain BaP degradation at different process variables. As can be seen from Table 2, relatively low δ value (time to the first decimal reduction) and C_{res} (residual BaP concentration) values were observed for BaP degradation using CDPJ generated at 1.5 A current and 15 mm STED.

Similar results were seen when BaP was degraded on glass slides and in food materials by low-pressure air plasma (LPAP) (Lee et al., 2019). In that study, among selected kinetic models (log-linear, log-linear tail, Weibull, and Weibull tail) to explain LPAP-induced BaP degradation, Weibull tail model was found to be the best model. Based on these results, it can be concluded that nonlinear modelling approaches can suitably explain the degradation pattern of BaP following non-thermal plasma treatment.

BaP degradation in food materials

Compared to untreated control samples, a significant (p<0.05) reduction in the levels of BaP in the seed samples was noted upon CDPJ treatment. The average initial levels of BaP in RRS, ORS, RRP, and ORP seeds were 8.51, 51.52, 9.87, and 77.27 μg/kg, respectively. After CDPJ treatment for 30 min, BaP levels in RRS, ORS, RRP, and ORP seeds were reduced by 42.61%, 45.90%, 41.31%, and 32.96%, respectively. Levels of BaP degradation (%) as a function of CDPJ treatment time in RRS, ORS, RRP, and ORP seeds are shown in Fig. 4. In the case of the seed oils, similar BaP degradation patterns were upon the plasma exposure. The average initial levels of BaP in regular roasted sesame oil (RRSO), over roasted sesame oil (ORSO), regular roasted perilla oil (RRPO) and over roasted perilla oil (ORPO) were 3.27, 21.44, 4.43 and 31.24 μg/kg, respectively. Following CDPJ treatment of RRS, ORS, RRP and ORP seeds for 30 min, the levels of BaP in RRSO, ORSO, RRPO and ORPO were decreased by 38.48, 38.37, 40.81 and 41.94%, respectively. Levels of BaP degradation (%) as a function of CDPJ treatment time in RRSO, ORSO, RRPO and ORPO are shown in Fig. 5.

In a previous study, the removal of pyrene and BaP from contaminated water by integrated ozonation-biological degradation techniques was shown (Yerushalmi et al., 2006). They found that, during the simultaneous treatment process (ozonation in the presence of microbial biomass), up to 91% overall removal of BaP following 30 minutes of ozonation (0.5 mg/L ozone); and, during the sequential treatment mode (ozonation as a pretreatment process), increasing to 100%

Table 1. Kinetic models tested for fitting of data obtained for CDPJ-induced BaP degradation

Model type	SSE	RMSE	R^2
Log linear	0.0171±0.0057	0.1291±0.0217	0.7243±0.0492
Log linear tail	0.0054±0.0011	0.0730±0.0078	0.9211±0.0178
Weibull	0.0007±0.0003	0.0258±0.0069	0.9902±0.0038
Weibull tail	0.0006±0.0003	0.0227±0.0073	0.9926±0.0041

SSE; sum of squared errors, RMSE; root mean squared error

Table 2. δ value (time to the first decimal reduction), C_{res} (residual BaP concentration) levels and curve shape factor values obtained for BaP degradation by CDPJ

Sample-to-electrode distance (mm)	Current (A)	δ value (min)	C_{res} (%)	Curve shape factor
15	1.00	44.51±4.18	12.31	0.42
	1.25	41.22±4.00	11.74	0.37
	1.50	37.34±5.27	10.47	0.39
25	1.00	75.78±12.56	19.05	0.38
	1.25	53.40±7.84	15.49	0.30
	1.50	51.69±9.05	13.48	0.43
30	1.00	163.13±19.72	20.41	0.32
	1.25	155.01±26.05	19.05	0.27
	1.50	76.30±8.74	16.59	0.30

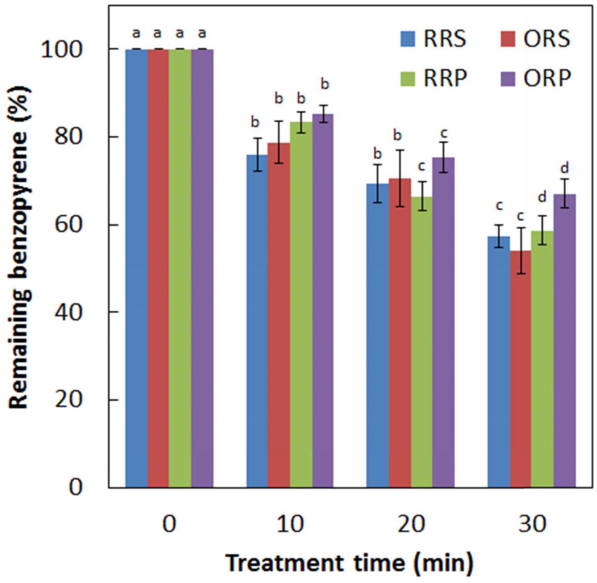

Fig. 4. Level of BaP degradation (%) as a function of CDPJ treatment time in regular roasted sesame (RRS), over roasted sesame (ORS), regular roasted perilla (RRP), and over roasted perilla (ORP) seeds. Different lower-case letters indicate statistically significant difference (p<0.05).

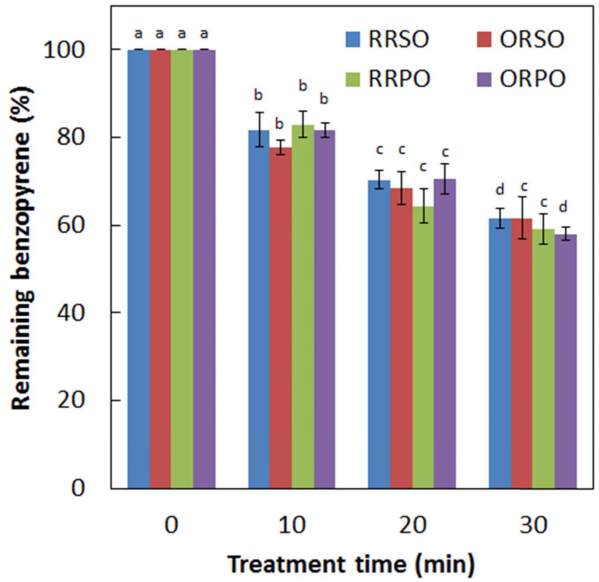

Fig. 5. Level of BaP degradation (%) as a function of CDPJ treatment time in regular roasted sesame oil (RRSO), over roasted sesame oil (ORSO), regular roasted perilla oil (RRPO) and over roasted perilla oil ORPO. Different lower-case letters indicate statistically significant difference (p<0.05).

overall removal following 60 min of ozonation (2.5 mg/L ozone). In another study, upon treatment with low-pressure cold plasma (168 W, 1.0 Torr pressure) for 30 min, initial BaP concentration on slides was reduced by 82.7% and by 40-46% in roasted sesame and perilla seeds (Lee et al., 2019). These studies indicate the potential of AOPs for BaP degradation.

The mechanism of BaP degradation seems complex and alter with the type of oxidizing agent. On the application of AOPs, radical reactions and direct reaction pathways have been shown to be predominant in the degradation of BaP in aqueous solution (Miller et al., 2002). Their study showed that radical reactions were prevalent in H_2O_2-based processes; and about 50% contribution by radical reactions was observed in a H_2O_2/UV system. On the contrary, direct reactions were prevalent in BaP degradation in a neutral aqueous solution following treatment using O_3 and O_3/UV systems. It was concluded that acidic conditions favored direct reaction pathways and basic conditions encouraged the radical mechanism of oxidation (Miller et al., 2002). The formation of epoxide products (mono-epoxides and diol-epoxides) upon heterogeneous reaction of BaP with gas-phase O_3 has been shown (Zhou et al., 2017).

BaP degradation products, which are formed as intermediates in the oxidative degradation of BaP, could pose a toxic risk. Diol-epoxides, which are formed during BaP oxidation by O_3, are known carcinogens (Zhou et al., 2017).

Summary

The plasma reaction conditions for BaP degradation were optimized. Under the optimal degradation conditions, the initial concentrations of BaP on slides were decreased by up to 87.09% in 30 min. The Weibull tail model was found to be best-fit model compared with others to explain the kinetics of BaP degradation by the plasma discharges. In the food samples, following the plasma treatment (at optimal conditions) for 30 min, the average levels of BaP degradation ranged between 32.96-45.90%. As gas plasmas are known to produce different reactive species, radical reactions or oxidation by radical mechanisms might have played a dominant role in BaP degradation.

Acknowledgements

This study was supported by the Ottogi Foundation, Korea (Grant No. 2016-0066) and Gachon University research fund of 2018 (GCU-2018-0675).

References

Albert I, Mafart P. 2005. A modified Weibull model for bacterial inactivation. Int. J. Food Microbiol. 100: 197-211.

Attri P, Yusupov M, Park JH, Lingamdinne LP, Koduru JR, Shiratani M, Choi EH, Bogaerts A. 2016. Mechanism and comparison of needle-type non-thermal direct and indirect atmospheric pressure plasma jets on the degradation of dyes. Sci. Rep. 6: 34419.

Bigelow WD, Esty JR. 1920. The thermal death point in relation to typical thermophylic organisms. J. Infect. Dis. 27: 602-617.

Chen YH, Xia EQ, Xu XR, Li S, Ling WH, Wu S, Deng GF, Zou ZF, Zhou J, Li HB. 2012. Evaluation of benzo[α]pyrene in food from China by high-Performance liquid chromatography-fluorescence detection. Int. J. Env. Res. Pub. He. 9: 4159-4169.

Cheng W, Liu G, Wang X, Liu X, Liu B. 2015. Formation of benzo(a)pyrene in sesame seeds during the roasting process for production of sesame seed oil. J. Am. Oil Chem. Soc. 92: 1725-1733.

Choi S, Puligundla P, Mok C. 2017. Impact of corona discharge plasma treatment on microbial load and physico-chemical and sensory characteristics of semi-dried squid (*Todarodes pacificus*). Food Sci. Biotechnol. 26: 1137–1144.

Fu PP, Xia Q. 2016. Food chemical carcinogens: sources and mechanism of exogenous DNA adduct formation. In: Food Toxicology, Debasis Bagchi and Anand Swaroop (eds.) Boca

Raton, Florida: CRC Press (pp. 57-81).

Geeraerd AH, Herremans CH, Van Impe JF. 2000. Structural model requirements to describe microbial inactivation during a mild heat treatment. Int. J. Food Microbiol. 59: 185-209.

Homem V, Dias Z, Santos L, Alves A. 2009. Preliminary feasibility study of benzo(a)pyrene oxidative degradation by Fenton treatment. J. Environ. Public Health Article ID 149034: 6 pages.

IARC. 2012. Benzo[α]pyrene. IARC Monographs on the evaluation of carcinogenic risks on humans. Volume 100F: 111-144. Available at https://monographs.iarc.fr/wp-content/uploads/2018/06/mono100F-14.pdf

Kim JW, Puligundla P, Mok C. 2015. Microbial decontamination of dried laver using corona discharge plasma jet (CDPJ). J. Food Eng. 161: 24-32.

Kot-Wasik A, Dabrowska D, Namiesnik J. 2004. Photodegradation and biodegradation study of benzo(a)pyrene in different liquid media. J. Photochem. Photobiol. A 168: 109-115.

Lee T, Puligundla P, Mok C. 2019. Degradation of benzo[α] pyrene on glass slides and in food samples by low-pressure cold plasma. Food Chem. 286: 624-628.

Mafart P, Couvert O, Gaillard S, Leguerinel I. 2002. On calculating sterility in thermal preservation methods: Application of the Weibull frequency distribution model. Int. J. Food Microbiol. 72: 107-113.

Miller JS, Olejnik D, Ledakowicz S. 2002. Role of radical reactions in benzo[α]pyrene degradation by advanced oxidation processes. Inzynieria Chemiczna i Procesowa 23: 151-171.

Miller KP, Ramos KS. 2001. Impact of cellular metabolism on the biological effects of benzo[α]pyrene and related hydrocarbons. Drug Metab. Rev. 33: 1-35.

Nam K, Kukor JJ. 2000. Combined ozonation and biodegradation for remediation of mixtures of polycyclic aromatic hydrocarbons in soil. Biodegradation 11: 1-9.

Ottinger SE, Mayura K, Lemke SL, McKenzie KS, Wang N, Kubena LF, Phillips TD. 1999. Utilization of electrochemically generated ozone in the degradation and detoxication of benzo[α]pyrene. J. Toxicol. Environ. Health. A 57: 565-583.

Puligundla P, Kim JW, Mok C. 2017. Effect of corona discharge plasma jet treatment on decontamination and sprouting of rapeseed (*Brassica napus* L.) seeds. Food Control 71: 376-382.

Wilson SC, Jones KC. 1993. Bioremediation of soil contaminated with polynuclear aromatic hydrocarbons (PAHs): A review. Environ. Pollut. 81: 229-249.

Yerushalmi L, Nefil S, Hausler R, Guiot SR. 2006. Removal of pyrene and benzo (a) pyrene from contaminated water by sequential and simultaneous ozonation and biotreatment. Water Environ. Res. 78: 2286-2292.

Zhou S, Yeung LWY, Forbes MW, Mabury S, Abbatt JPD. 2017. Epoxide formation from heterogeneous oxidation of benzo[α]pyrene with gas-phase ozone and indoor air. Environ. Sci. Process. Impact. 19: 1292-1299.